

without linear constraints and the detection of gross errors in process data as a problem of testing for outliers in statistical data. The proposed gross error detection scheme makes use of a recently-developed test which possesses maximal power properties for detecting the presence of a single outlier (gross error). This test can be extended to deal with multiple outliers but without the guarantee of maximal power properties. The procedure which is applicable to any linear reconciliation problem is simple to apply and to program on computers.

For process data obeying normal distribution but containing a single gross error the power of this test is given in closed analytical form. Its properties for a more realistic situation may be obtained by computer simulation.

By dealing directly with the residuals (the differences between observed and fitted values) the necessity of interposing an identification scheme following the detection of one or more gross errors is eliminated. Once a gross error is detected, its origin is automatically identified.

Acknowledgment

Partial support of this work was provided by the National Science Foundation Grant CPE 76-18852.

NOTATION

A	= a ($q \times p$) matrix of known constants
b	= a ($p \times 1$) vector of unknown parameters
\hat{b}	= least-squares estimate of \hat{b}
\hat{b}_0	= the unconstrained least-squares estimate of \hat{b}
c	= a ($q \times 1$) vector of known constants
d	= a transformed residual vector defined by Eq. (13)
D	= an ($n \times p$) matrix of known constants
e	= the residuals $\underline{y} - \hat{\underline{y}}$
$E(\cdot)$	= expected value of
G	= $Q^{-1}(\underline{I} - \underline{DM})$
I	= identity matrix
k	= $Z_{\beta/2}$, the $(1 - \beta/2)$ th quantile of the standard normal distribution
M	= a ($p \times n$) matrix defined by Eq. (7)
n	= the number of measured variables

N	= a ($p \times q$) matrix defined by Eq. (8)
p	= the number of unknown parameters
$P\{\cdot\}$	= probability of
q	= the number of linear constraints
Q	= an ($n \times n$) variance-covariance matrix
V	= variance-covariance matrix of the residuals, \underline{e}
W	= variance-covariance matrix of transformed residuals, \underline{d}
y	= an ($n \times 1$) vector of measured variables
\hat{y}	= an ($n \times 1$) vector of adjusted measurements
Z_i	= a test statistic defined by Eq. (15)
Z'_i	= a test statistic defined by Eq. (12)
α	= level of significance
β	= modified level of significance defined by Eq. (18)
δ_i	= a gross error
ϵ	= an ($n \times 1$) vector of errors
ν_i	= the expected value of Z
Φ	= standard normal distribution function, Eq. (23)

LITERATURE CITED

- Almasy, G. A., and T. Sztano, "Problems of Control and Information Theory," 4, (1), 57 (1975).
- Barnett, V., and T. Lewis, *Outliers in Statistical Data*, John Wiley, New York (1978).
- Madron, F., V. Veverka and V. Vanecek, *AIChE J.*, 23, 482 (1977).
- Mah, R. S. H., "Design and Analysis of Process Performance Monitoring Systems," Proceedings of the Engineering Foundation Conference on "Chemical Process Control II," Sea Island, GA, (Jan. 18-23, 1981).
- Mah, R. S. H., G. M. Stanley, and D. M. Downing, *Ind. Eng. Chem. Proc. Des. Dev.*, 15, 175 (1976).
- Murthy, A. K. S., *Ind. Eng. Chem. Proc. Des. Dev.*, 12, 246 (1973).
- Murthy, A. K. S., *ibid.*, 13, 347 (1974).
- Nogita, S., *Ind. Eng. Chem. Proc. Des. Dev.*, 11, 197 (1972).
- Romagnoli, J. A., and G. Stephanopoulos, *Chem. Eng. Sci.*, 35, 1067 (1980).
- Seber, G. A. F., *Linear Regression Analysis*, John Wiley, New York (1977).
- Sidak, Z., *J. Amer. Statist. Assoc.*, 62, 626 (1967).
- Tamhane, A. C., "A Note on the Use of Residuals for Detecting an Outlier in Linear Regression," to appear in *Biometrika*.

Manuscript received August 10, 1981; revision received December 11, and accepted January 13, 1982.

Laminar Flow in the Entrance Region of a Parallel Plate Channel

A. K. MOHANTY and REETA DAS

Department of Mechanical Engineering
Indian Institute of Technology
Kharagpur, India

Fluid flow in the entrance region of a channel, or a pipe is characterized by non-similar velocity profiles. Typically, a length of 150 diameters may exist in a laminar flow at Reynolds number equal to 2,000, before the fully developed Poiseuille profile is established. It is quite possible, therefore, that in a large majority of practical applications, such as in connecting pieces or in heat exchangers, of much interest to chemical engineers, the transport phenomena are confined to the entrance region.

The problem of laminar flow in the entrance region of pipes and ducts has been studied extensively by several investigators, e.g.,

Schiller (1922), Schlichting (1979), Wang and Longwell (1964). These investigations were based, primarily, on the assumption that fully developed velocity profile is established at the location where the boundary layers meet at the duct axis. However, in a recent study of flow through a circular pipe (Mohanty and Asthana, 1979), it has been shown, both analytically and experimentally, that the boundary layers meet much earlier and the velocity profile undergoes adjustment in a purely viscous region to finally attain the fully developed form. The boundary layer region is called the "inlet region," and the viscous zone the "filled region," after Shingo (1966).

The present study is aimed at extending the inlet and filled region model to a parallel plate channel.

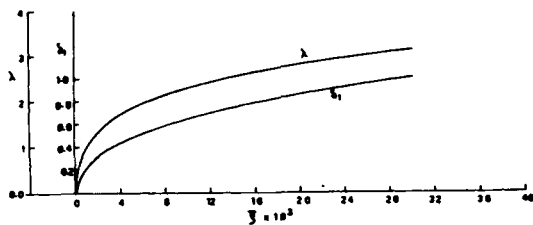


Figure 1. Boundary layer thickness and pressure gradient parameter in the inlet region.

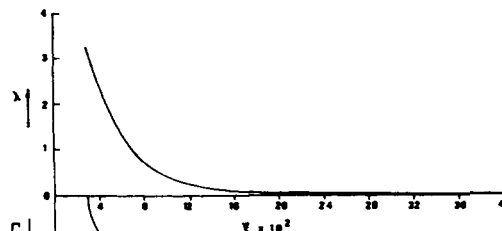


Figure 2. Pressure gradient parameters in the filled region.

ANALYSIS

The circular pipe results indicate that the filled region is about three times as long as the boundary layer zone. Order of magnitude analysis is, hence, considered applicable to both the inlet and the filled regions.

Choosing a rectangular coordinate system the conservation equations for both the inlet and filled regions are:

$$\frac{\partial u}{\partial x} + \frac{\partial v}{\partial y} = 0 \quad (1)$$

$$u \frac{\partial u}{\partial x} + v \frac{\partial u}{\partial y} = -\frac{1}{\rho} \frac{\partial p}{\partial x} + \nu \frac{\partial^2 u}{\partial y^2} \quad (2)$$

$$0 = \frac{\partial p}{\partial y} \quad (3)$$

The boundary conditions common to both regions are:

$$(i) \quad u = v = 0 \quad \text{at} \quad y = 0$$

$$(ii) \quad u = U_{\infty}(x) \quad \text{at} \quad y = \delta$$

$$(iii) \quad \frac{\partial u}{\partial y} = 0 \quad \text{or} \quad y = h.$$

In the inlet region, the free stream condition further requires

$$(iv) \quad \frac{\partial^2 u}{\partial y^2} = 0 \quad \text{at} \quad y = \delta.$$

In the filled region $(\partial^2 u / \partial y^2)_{y=h}$ cannot be assigned a definite value due to the absence of a potential core.

We, therefore, define

$$\left(\frac{\partial^2 u}{\partial y^2} \right)_{y=h} = \frac{U_c \Gamma}{h^2},$$

where Γ is to be otherwise evaluated.

The momentum equation at the wall is

$$\left(\frac{\partial u}{\partial y^2} \right)_{y=0} = \frac{1}{\mu} \frac{dp}{dx}$$

The pressure gradient, on the other hand, is evaluated from the same equation at $y = \delta$ in the inlet, and $y = h$ in the filled region, and its general form is:

$$\frac{dp}{dx} = -\rho U_c \frac{dU_c}{dx} + \mu \left(\frac{\partial^2 u}{\partial y^2} \right)_{y=h} \quad (4)$$

Note, for example, that Eq. 4 yields the Bernoulli's pressure gradient in the boundary layer zone where $(\partial^2 u / \partial y^2)_{y=\delta}$ is zero. Using further the definition of λ and Γ , we write a 5th boundary condition as;

$$(v) \quad \left(\frac{\partial^2 u}{\partial y^2} \right)_{y=0} = \frac{U_c}{h^2} (\Gamma - \lambda).$$

The above form is applicable in the inlet region with

$$\Gamma = 0, \quad U_c = U_{\infty}, \quad h = \delta.$$

The velocity profile satisfying these five boundary conditions has the general form

$$\begin{aligned} \bar{u} = & (2\eta - 2\eta^3 + \eta^4) + \frac{\lambda}{6} (\eta - 3\eta^2 + 3\eta^3 - \eta^4) \\ & + \frac{\Gamma}{2} (\eta^2 - 2\eta^3 + \eta^4) \quad (5) \end{aligned}$$

The velocity profile given by Eq. 5 satisfied the fully developed condition $\bar{u} = 2\eta - \eta^2$, when $\lambda = 0$, and $\Gamma = -2$. In other words, $\lambda = 0$, $\Gamma = -2$ values mark the end of the filled as well as the entrance region.

SOLUTION

Karman-Pohlhausen type integral analysis (1921; see Schlichting, 1979, p. 206) is carried out by integrating the momentum Eq. 2 from 0 to δ in the inlet region and 0 to h in the filled region, eliminating ϑ by the application of continuity Eq. 1. The resultant form is

$$\frac{d\delta^{**}}{dx} + (2\delta^{**} + \delta^*) \frac{v\lambda}{h^2 U_c} - \frac{v}{h} \cdot \frac{\Gamma}{U_c} = \frac{C_f}{2} \quad (6)$$

The area averaged continuity equation is expressed through displacement thickness as:

$$\frac{U_{\infty}}{U_c} = \frac{1}{(1 - \delta_1^*)} \quad (7)$$

where U_{∞} is substituted by U_c in the filled region.

In order to avoid any approximation in the treatment of conservation of mass, such as was adopted by Schlichting (1979, p. 185) by expanding Eq. 7 in a finite series, we adopt, after Mohanty & Asthana (1979), the differential form of Eq. 7 for simultaneous solution with the momentum Eq. 6.

The resulting equations are:

Inlet region: $\delta_1 \leq 1, \gamma = 0$

$$\frac{d\delta_1}{d\xi} = (F_3 F_5 - F_6 F_2) / (F_1 F_5 - F_2 F_4)$$

$$\frac{d\lambda}{d\xi} = (F_4 F_3 - F_1 F_6) / (F_1 F_5 - F_2 F_4) \quad (8)$$

Filled region: $\delta_1 = 1, U_{\infty} = U_c$

$$\frac{d\lambda}{d\xi} = (2F_9 - F_8 F_{10}) / (2F_7 - F_8)$$

$$\frac{d\Gamma}{d\xi} = (F_7 F_{10} - F_9) / (2F_7 - F_8) \quad (9)$$

The functions F_1 to F_{10} are defined in the appendix. Eqs. 8 and 9 are solved numerically using fourth order Runge-Kutta method. Approximating on the basis of the flat plate boundary layer results, and by trials and errors, the initial values for stable numerical computation are taken as:

$$\xi = 0.0001, \quad \delta_1 = 0.02, \quad \lambda = 0.017$$

RESULTS AND CONCLUSIONS

The sets of Eqs. 8 and 9 represent simultaneous treatment of conservations of mass and momentum in the inlet and filled regions.

The value of $\delta_1 = 1.00$ attained at $\xi = 0.0293$ marks the end of the inlet region; the pressure gradient value being $\lambda = 3.1090$. This value of λ , and $\Gamma = 0$ are the initial values for the filled region solutions.

Ninety-nine percent of Poiseuille value for (U_c/U_o) is reached at $\xi = 0.1100$, where $\lambda = 0.35$ and $\Gamma = -1.820$, whereas 99% of the skin friction value is attained at $\xi = 0.1301$. Taking the 99% velocity value as the index of fully developed condition the entrance length for the parallel plate channel is 0.11. Considering that the entrance length is made up of inlet and filled regions, the length of the filled region is 0.081.

The variation of δ_1 , λ and Γ are plotted in Figures 1 and 2.

In terms of λ and Γ , the non-dimensional pressure gradient is expressed, using Eq. 4 as

$$\frac{dp^*}{d\xi} = -4(\lambda - \Gamma)/(1 - \delta_1^*) \quad (10)$$

The calculated values of δ , λ , Γ , U_c/U_o , C_f , C_{f1} and $(dp^*/d\xi)$ are tabulated together with the results of Goldstein (1965) for pressure gradient. The exact values noted at the end of Table 1 are obtained for the Poiseuille flow.

ACKNOWLEDGMENT

Extension of a research scholarship to one of the authors (RD) by the Indian Space Research Organization and the coordination of Prof. R. S. Nanda for the ISRO grant are gratefully acknowledged.

NOTATION

C_f	= skin friction coefficient = $\tau_w/1/2\rho U_\infty^2$ or $\tau_w/1/2\rho U_c^2$
C_{f1}	= $\tau_w/1/2\rho U_o^2$
h	= half width of the parallel-plate channel
p	= pressure
p_o	= pressure at inlet
p^*	= $(p_o - p)/1/2\rho U_o^2$
Re	= Reynolds number = $(U_o 2h)/\nu$
u	= axial velocity
U_o	= average velocity
U_∞	= free stream velocity in the inlet region
U_c	= centre line velocity in the filled region

\bar{u}	= dimensionless velocity $\frac{u}{U_\infty}$ or $\frac{u}{U_c}$
x	= axial coordinate
y	= transverse coordinate measured from channel wall

Greek Letters

δ	= boundary layer thickness $\delta_1 = \delta/h$
δ^*	= displacement thickness = $\int_0^\delta (1 - \bar{u}) dy$
δ^{**}	= momentum thickness = $\int_0^\delta \bar{u}(1 - \bar{u}) dy$
δ_1^*	= δ^*/h , $\delta_1^{**} = \delta^{**}/h$
η	= dimensionless coordinate $\frac{y}{\delta}$ or $\frac{y}{h}$
λ	= pressure gradient parameters = $\frac{\delta^2}{\nu} \frac{dU_\infty}{dx}$ or $\frac{h^2}{\nu} \frac{dU_c}{dx}$
Γ	= pressure gradient parameter in the filled region = $\left(\frac{\partial^2 u}{\partial y^2}\right)_{y=h} \cdot \frac{h^2}{U_c}$
μ	= dynamic viscosity
ν	= Kinematic viscosity
φ	= density
τ_w	= wall shear stress
ξ	= dimensionless axial distance = $x/(h \cdot Re)$

Appendix

Inlet

$$F_1(\lambda, \delta) = \delta_1 \left(\frac{37}{315} - \frac{\lambda}{945} - \frac{\lambda^2}{9,072} \right)$$

$$F_2(\lambda, \delta) = \delta_1^2 \left(\frac{1}{945} + \frac{\lambda}{4,536} \right)$$

$$F_3(\lambda, \delta) = \left(4 - \frac{232\lambda}{315} + \frac{79\lambda^2}{3,780} + \frac{\lambda^3}{2,268} \right) + \delta_1 \left(\frac{\lambda^4}{272,160} + \frac{19\lambda^3}{453,600} - \frac{469\lambda^2}{37,800} + \frac{267\lambda}{1,050} - \frac{6}{5} \right)$$

$$F_4(\lambda, \delta) = \delta_1^2 \left(\frac{3}{10} - \frac{\lambda}{120} \right), F_5(\lambda, \delta) = \frac{\delta_1^3}{120}$$

$$F_6(\lambda, \delta) = 2\lambda + \delta_1 \left(\frac{\lambda^2}{30} - \frac{6\lambda}{5} \right) + \delta_1^2 \left(\frac{9\lambda}{50} - \frac{\lambda^2}{100} + \frac{\lambda^3}{7,200} \right)$$

TABLE 1. SALIENT RESULTS: INLET REGION

$\xi = \frac{x}{(h \cdot Re)}$	δ_1 (Inlet)/ Γ (Filled)	λ	$\frac{U_c}{U_o}$	$C_f \frac{Re}{4}$	$C_{f1} \frac{Re}{4}$	$\frac{p_o - p}{(1/2)\rho U_o^2}$	$\frac{p_o - p}{(1/2)\rho U_o^2}$ (Goldstein)
0.0001	0.0216	0.1084	1.0065	92.7680	93.9790	0.0130	—
0.0005	0.1568	0.7137	1.0484	12.8899	14.1661	0.0990	0.1100
0.0010	0.2284	0.9942	1.0714	8.8476	10.1562	0.1479	0.1600
0.0100	0.6534	2.3071	1.2247	2.9798	4.4693	0.4993	0.5100
0.0250	0.9407	2.9833	1.3493	1.9674	3.5815	0.8203	0.7720
0.0290	0.9951	3.0985	1.3753	1.8387	3.4775	0.8912	—
0.0293	1.0000	3.1090	1.3776	1.8276	3.4687	0.8979	—
Filled Region							
0.0401	-0.7380	2.5769	1.4102	1.7229	3.4258	1.1066	1.0020
0.0806	-1.5989	0.7920	1.4708	1.4496	3.1355	1.7507	—
0.1004	-1.7655	0.4601	1.4827	1.4005	3.0792	2.0199	—
0.1103	-1.8203	0.3520	1.4860	1.3846	3.0608	2.1492	— (99% of U_c/U_o Value)
0.1301	-1.8940	0.2070	1.4923	1.3634	3.0358	2.4009	— (99% of C_{f1} Value)
0.2003	-1.9834	0.0322	1.4988	1.3380	3.0056	3.2605	—
0.2507	-1.9956	0.0085	1.4997	1.3345	3.0014	3.8677	3.6010
0.3956	-1.9999	0.0001	1.5000	1.3333	3.0000	5.6073	—
Exact	(-2.0000)	(0.0000)	(1.5000)	(1.3333)	(3.0000)		(Poiseuille Value)

$$\begin{aligned}
 F_7(\lambda, \Gamma) &= -\left(\frac{1}{945} + \frac{\lambda}{4,536} + \frac{\Gamma}{3,024}\right) \\
 F_8(\lambda, \Gamma) &= -\left(\frac{11}{1,260} + \frac{\lambda}{3,024} + \frac{\Gamma}{1,260}\right) \\
 F_9(\lambda, \Gamma) &= \left(\frac{14}{5} + \frac{22\Gamma}{15} - \frac{4,557\lambda}{9,450} + \frac{\Gamma^2}{30}\right) + \Gamma\lambda\left(\frac{493}{9,450} \right. \\
 &\quad \left. + \frac{167\lambda}{88,200} + \frac{17\Gamma}{7,560} + \frac{\Gamma\lambda}{28,350} + \frac{\lambda^2}{54,432} + \frac{\Gamma^2}{37,800}\right) \\
 &\quad + \lambda^2\left(\frac{107}{12,600} + \frac{73\lambda}{151,200} + \frac{\lambda^2}{272,160}\right) \\
 F_{10}(\lambda, \Gamma) &= -\left(\frac{294\lambda}{5} + \frac{\lambda^3}{120} + \frac{\Gamma^2\lambda}{30} + \frac{7\lambda^2}{5} + \frac{14\Gamma\lambda}{5} + \frac{\Gamma\lambda^2}{30}\right)
 \end{aligned}$$

- Goldstein, S., "Modern Developments in Fluid Dynamics," Oxford University Press, p. 310, (1965).
- Mohanty, A. K., and S. B. L. Asthana, "Laminar Flow in the Entrance Region of a Smooth Pipe," *J. Fluid Mech.*, **90**, 433 (1979).
- Schiller, L., "Die Entwicklung der Laminaren Geschwindigkeitsverteilung und ihr Bedeutung für Zähigkeitsmessungen," *ZAMM*, **2**, 96 (1922).
- Schlichting, H., "Boundary Layer Theory," 7th ed., p. 185 and p. 206, McGraw Hill Book Co., New York (1979).
- Shingo, "The Axi-Symmetric Laminar Flow in an Arbitrary Shaped Narrow Gap," *Bulletin J.S.M.E.*, **9**, No. 83,66 (1966).
- Wang, Y. L., and P. A. Longwell, "Laminar Flow in the Inlet Section of Parallel Plates," *AIChE J.*, **10**, 323 (1964).

Manuscript received February 12, 1981; revision received May 22, and accepted June 22, 1981.

Enthalpy of Hydrogen-Containing Hydrocarbon Liquids

The partial enthalpy of dissolved hydrogen in hydrocarbon liquids is derived from the fugacity correlation of Sebastian et al. and the results are presented in general equations. The partial enthalpy of the hydrocarbon solvent is found to be changed only insignificantly by the dissolved hydrogen from that of the pure liquid at the experimental conditions of up to 30 MPa in pressure.

H. Y. KIM, H. M. SEBASTIAN,
H. M. LIN, and K. C. CHAO

School of Chemical Engineering
Purdue University
West Lafayette, IN 47907

Large quantities of hydrogen are dissolved in liquid oils in hydrofining processes, sometimes to the extent of 50 mole % or higher in the liquid at the prevailing high temperature and high pressure, both of which tend to favor the solubility of hydrogen. Contrary to ordinary heavier gases, the partial molal enthalpy of solution of hydrogen is positive and large—in the order of several thousand calories per gram mole. The high solubility and large molal heat of solution mean that the total heat absorbed in the dissolution process can be substantial. The enthalpy of solution of hydrogen and the enthalpy change of the solvent due to the dissolved hydrogen are therefore of interest in process engineering. But these quantities cannot be calculated by conventional procedures based on pseudo-reduced correlations because of the peculiar properties of hydrogen as a quantum gas—extremely light molecular weight, low critical temperature, and small energies of interaction with other molecules.

An alternate approach to the enthalpy of hydrogen-containing liquids is to sum the partial molal enthalpy of the dissolved hydrogen and that of the solvent

$$\bar{H}_M = x_H \bar{H}_H + x_S \bar{H}_S \quad (1)$$

The symbols are explained in Notation.

Chueh and Deal (1973) developed general equations for the calculation of the partial enthalpies of Eq. 1. Henry constant of hydrogen at various temperatures was differentiated with respect to temperature to give the partial enthalpy of solution of hydrogen at infinite dilution. Correction terms were introduced for the effect of the finite concentration of hydrogen and for the effect of pressure in excess of the vapor pressure of the solvent. Chueh and Deal's contribution was the best then available, but the experimental data base of their correlation was limited, being made up of light solvents of the paraffins (up to n-octane), olefins (up to propylene), and aromatics (up to toluene).

Sebastian et al. (1981) recently developed a correlation of the fugacity of dissolved hydrogen at temperatures from 310 to 700 K and pressures to 30 MPa. The correlation was based on extensive experimental gas solubility data in hydrocarbons of a variety of molecular types including paraffins, mono- and poly-nuclear aromatics, naphthenes, and hetero-atom containing hydrocarbons. The ranges of temperature, pressure and solvent were all substantially extended from those of Chueh and Deal. Sebastian's correlation is applied for the derivation of the partial enthalpies reported here.

PARTIAL MOLAL ENTHALPY OF DISSOLVED HYDROGEN

The partial molal enthalpy of dissolved hydrogen is derived from the fugacity of the dissolved hydrogen upon differentiation with respect to temperature at constant pressure and composition

$$\frac{\bar{H}_H^* - \bar{H}_H}{RT^2} = \left[\frac{\partial \ln(f/x)}{\partial T} \right]_{p,x} \quad (2)$$

The symbols are explained in Notation.

Substituting the fugacity equation of Sebastian et al. (1981) into Eq. 2, we obtain

$$\frac{\bar{H}_H^* - \bar{H}_H}{RT^2} = g_1 + g_2 \frac{d\bar{\delta}}{dT} + g_3 \frac{p}{RT} + g_4 \frac{p}{RT} \frac{d\bar{\delta}}{dT} \quad (3)$$

The g 's in Eq. 3 are functions of temperature T and solubility parameter of the solution $\bar{\delta}$ given below.

$$g_1 = A_2/\bar{\delta} + A_3 + A_4\bar{\delta} + 2A_5\bar{\delta}^2T - 2A_6\bar{\delta}^2/T^3 \quad (4)$$

$$g_2 = -A_2T/\bar{\delta}^2 + A_4T + 2A_5T^2\bar{\delta} + 2A_6\bar{\delta}/T^2 \quad (5)$$

$$g_3 = -B_1/T + B_3T - B_4\bar{\delta}/T - B_5\bar{\delta}^2/T \quad (6)$$

$$g_4 = B_4 + 2B_5\bar{\delta} + B_6T \quad (7)$$

The coefficients A 's and B 's of Eqs. 4 to 7 are given in Table 1,